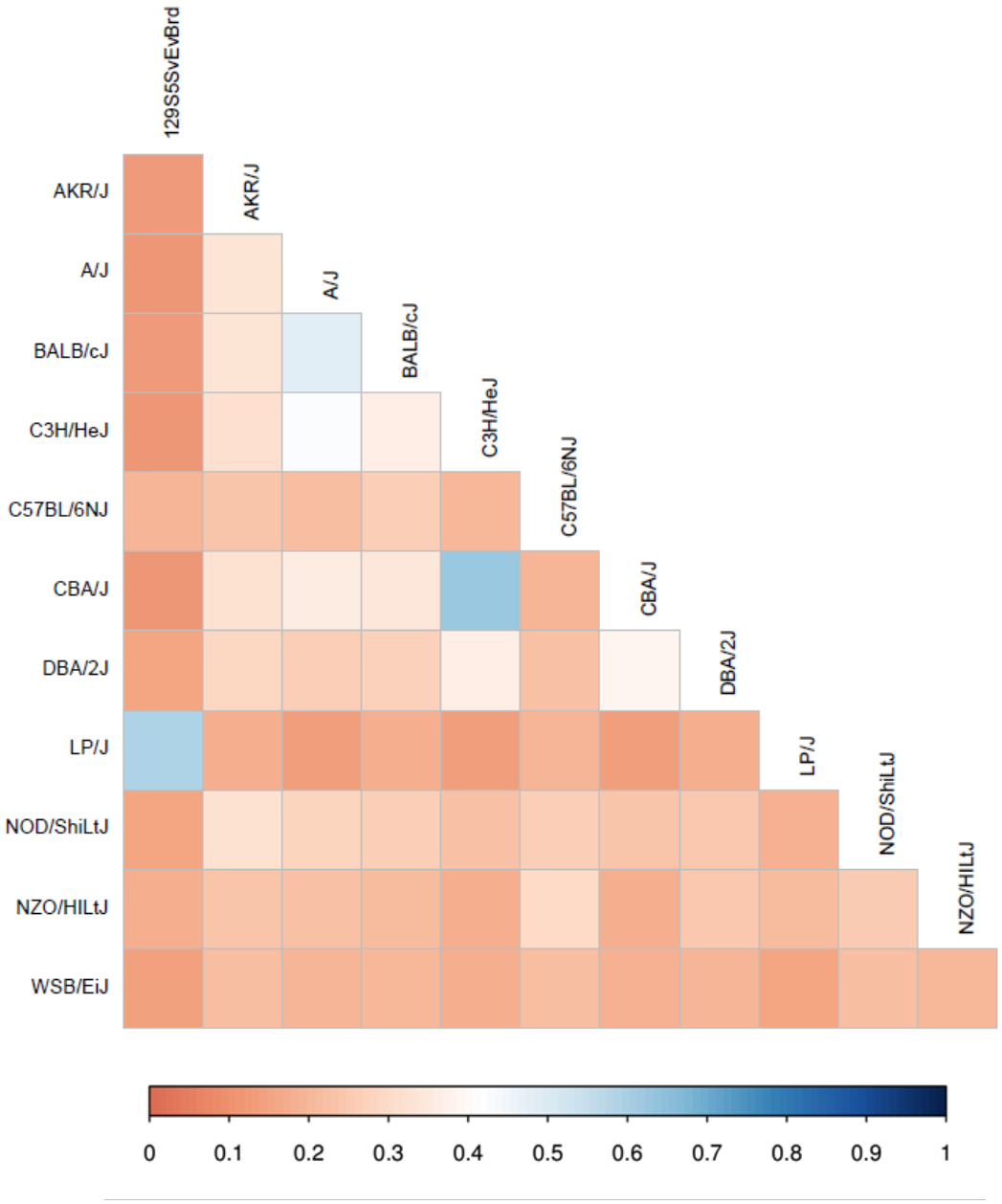

Figure S1 Genetic correlations between the 12 inbred strains. The correlations (Pearson correlation *r*) were calculated using a sample of 10% of all polymorphic SNPs. The legend bar shows the degree of correlation. The average correlation between strains is 0.2, with a range between 0.06 and 0.67.

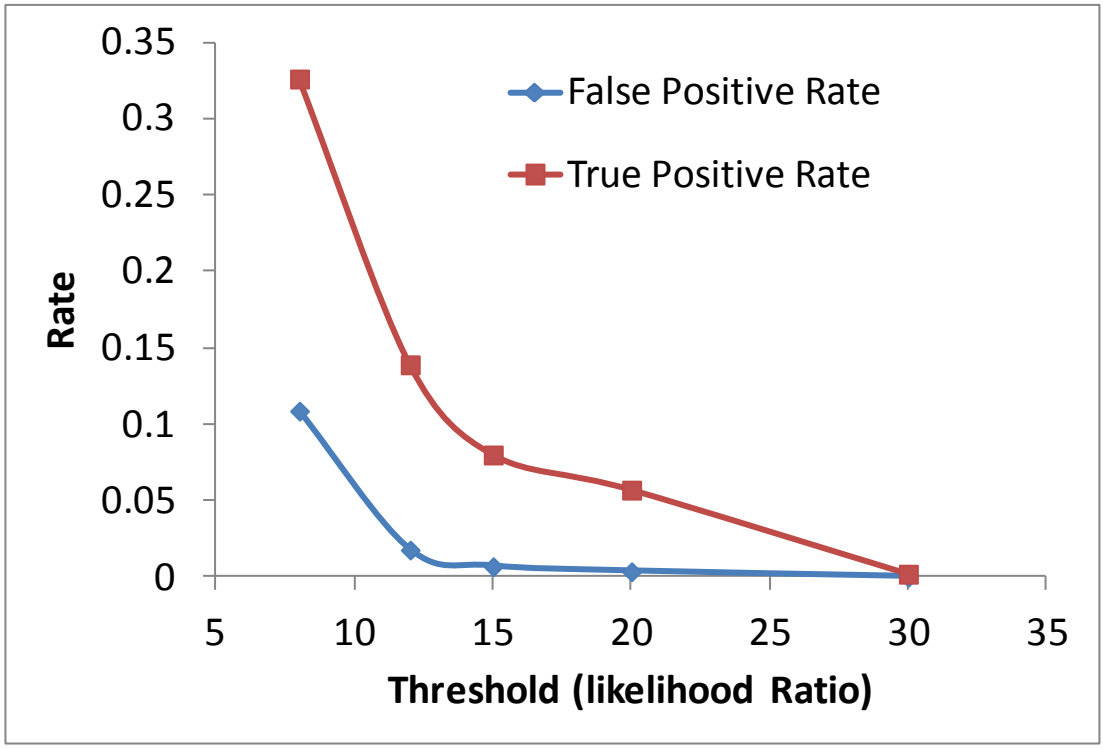

Figure S2 Hotspots detection performance on a simulated sample of 12 inbred lines. False positive and true positive rate are reduced as a function of more stringent threshold to declare hotspots.

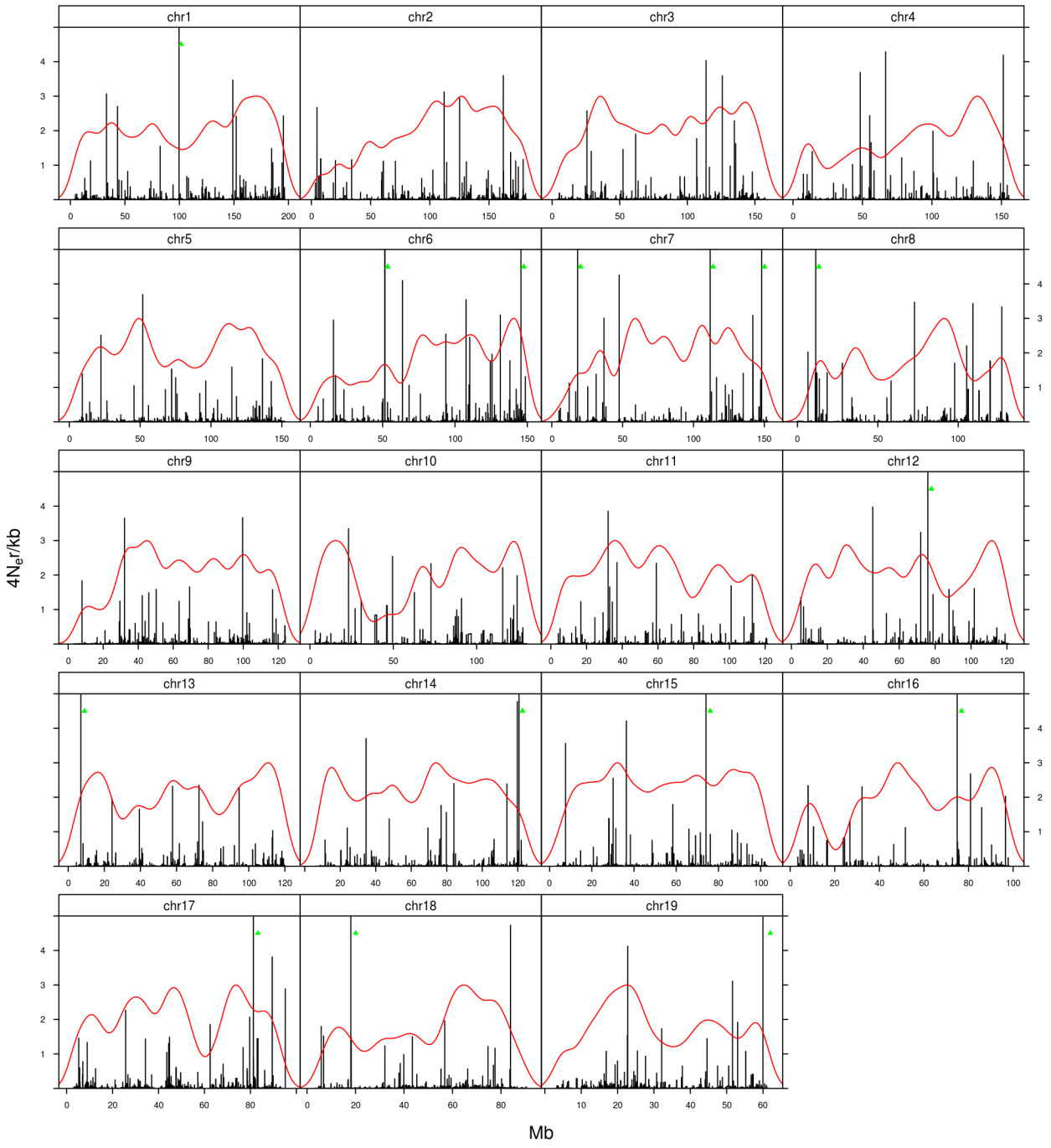

Figure S3 Recombination rates and SNP density for each chromosome. Recombination rates in terms of $4N_er$/kb are shown in black across each chromosome. Green triangles denote recombination rates which are higher than 5 $4N_er$/kb and are not fully shown for clarity purposes. The overlaying red line is the SNP density across the chromosome. The density of SNPs is approximately uniform in each chromosome.

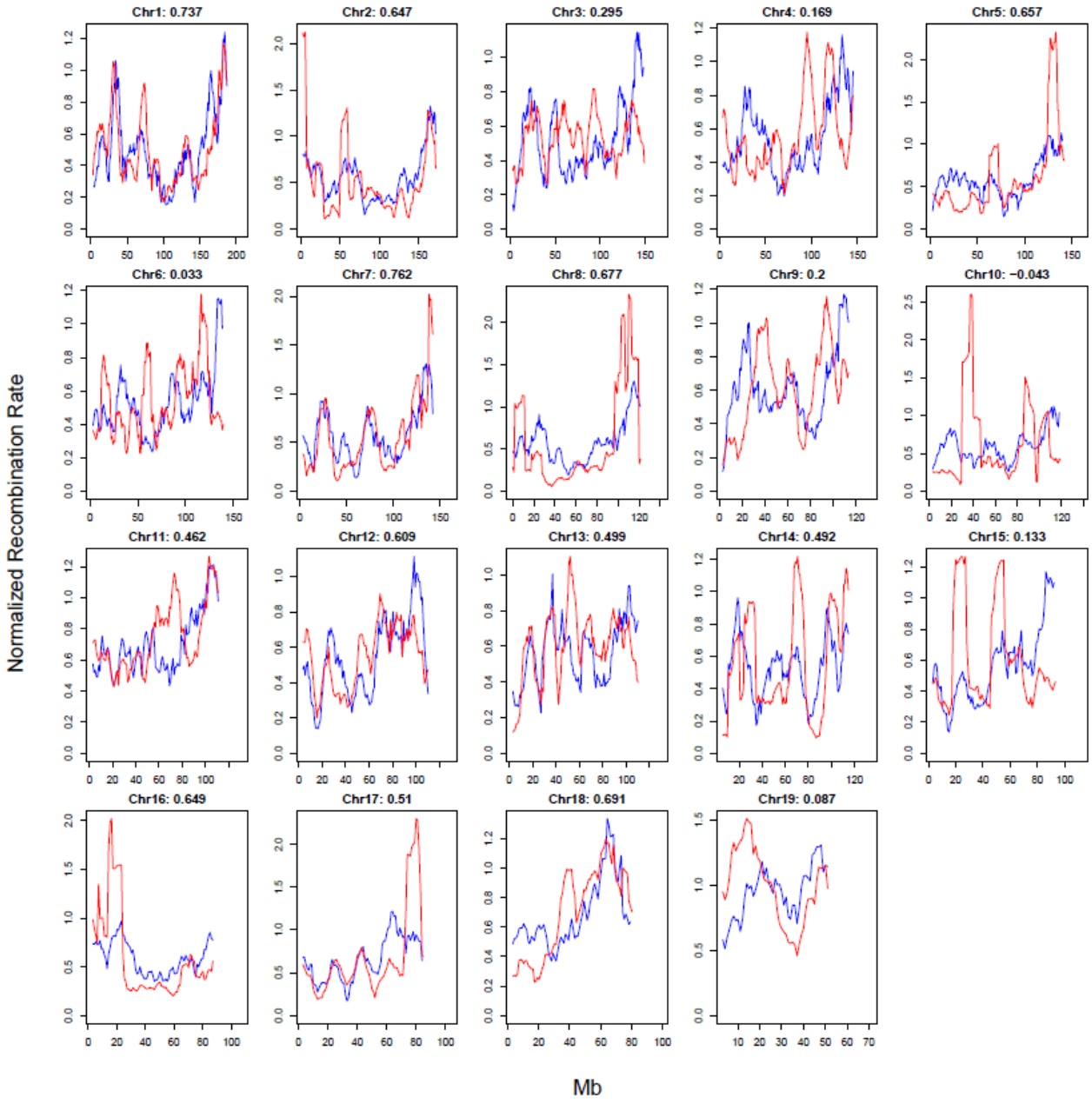

Figure S4 Recombination rates for each chromosome estimated by LDhat (red lines) and based on Cox et al. [S1] genetic map (blue lines). Rates were smoothed over 10 Mb with a shift of 1 Mb. We scaled the the LDhat map according to the Cox et al. map and then recalculated recombination rates as $(4N_{e}r)^{scaled}$/Mb (see also Materials and methods).

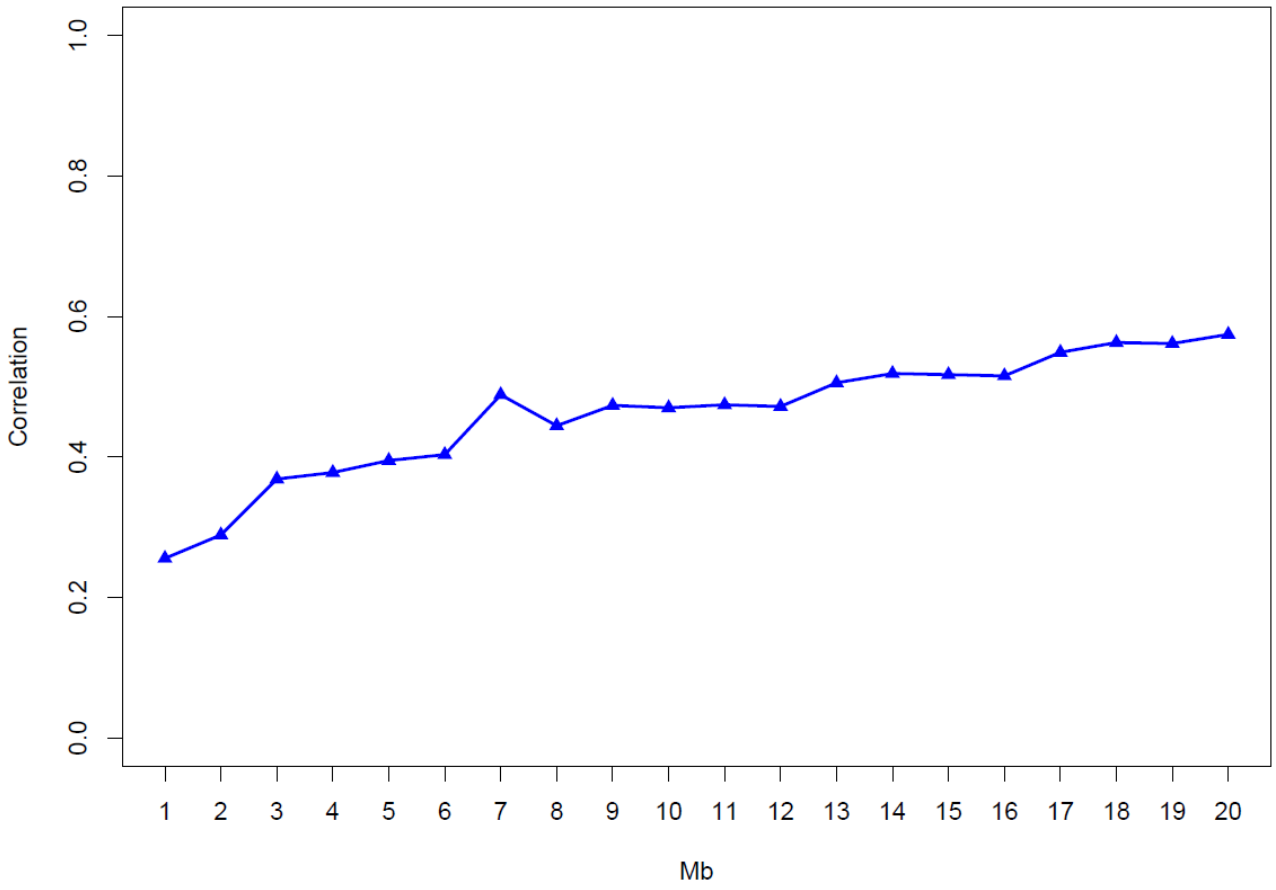

Figure S5 Correlations of the recombination rates estimated from mouse crosses (Cox et al. [S1]) and rates estimated from mouse inbred strains genetic data. The correlations (y-axis) are shown as a function of the window size in Mb (x-axis). The correlations were calculated with different sizes of non-overlapping windows.

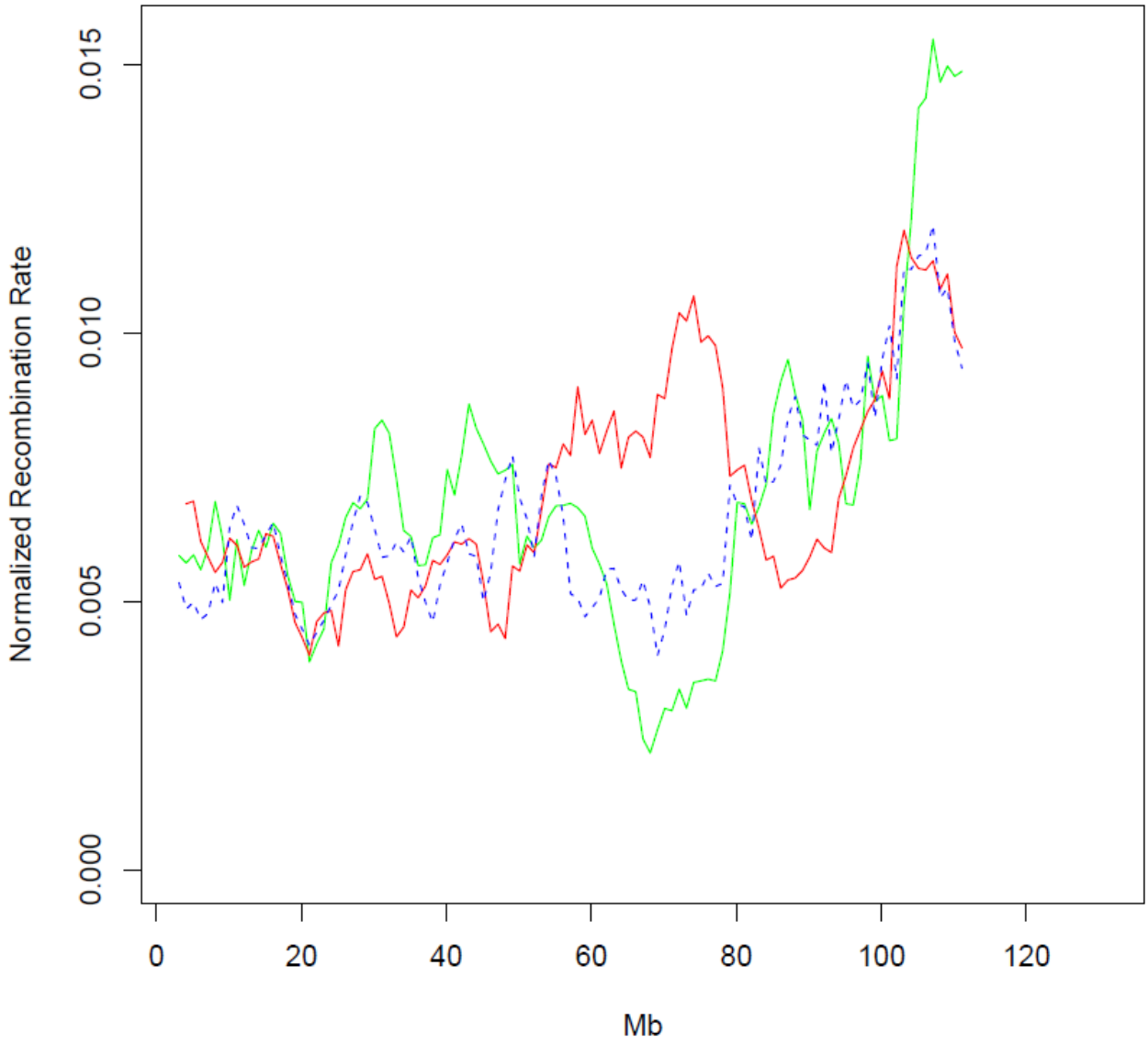

Figure S6 Recombination rates estimated by LDhat (red) and based on Billings et al. [S3] (green). As a comparison we also included the Cox et al. [S1] genetic map (blue dashed line). Rates were smoothed over a window of 10 Mb with a shift of 1 Mb. It can be seen that all three maps have similarities at different positions (see also the correlations in Figure S5). The calculation of the normalized recombination rates is described in Materials and methods.

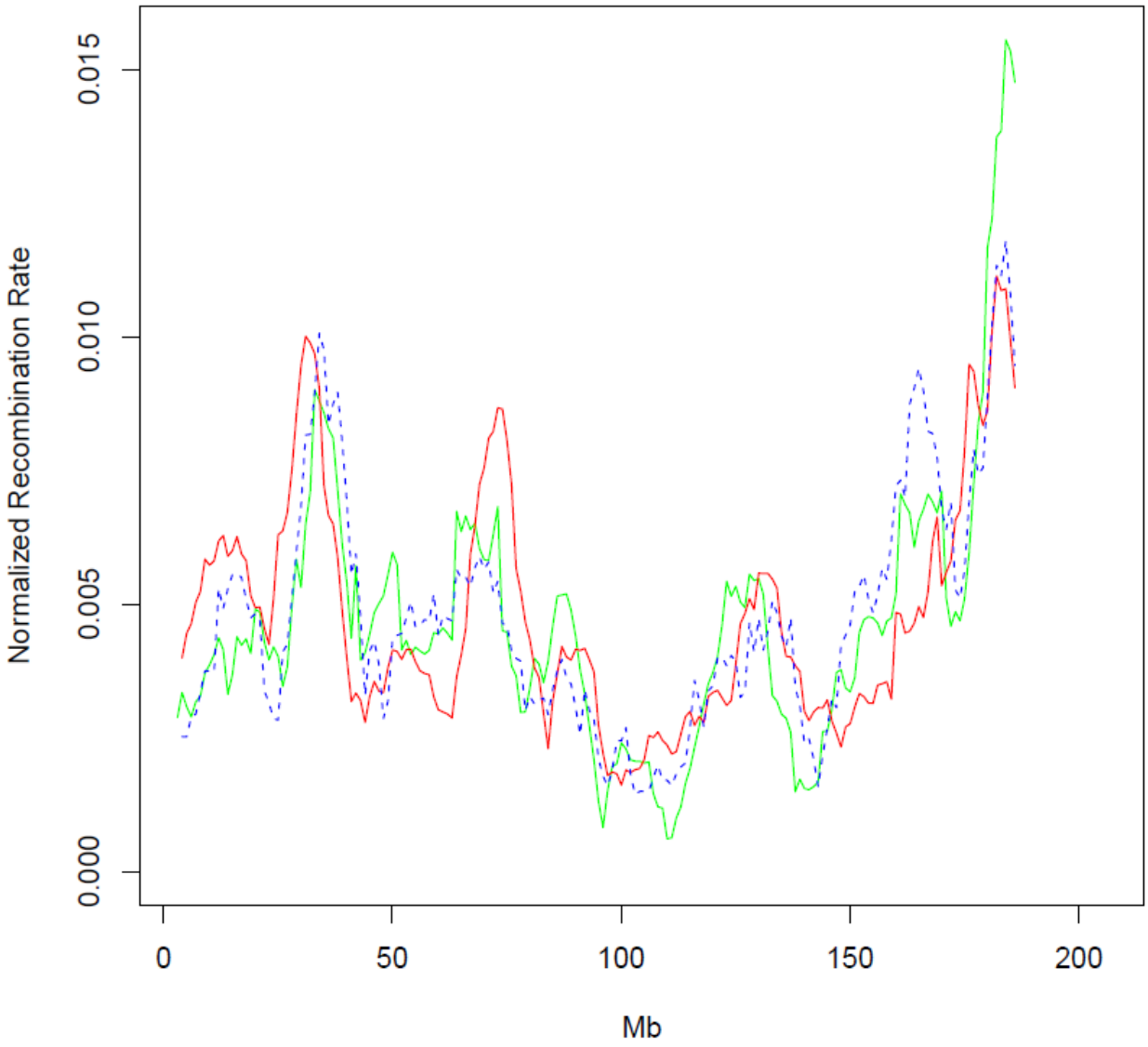

Figure S7 Recombination rates estimated by LDhat (red) and based on Paigen et al. [S2] (green). As a comparison we also included the Cox et al. [S1] genetic map (blue dashed line). Rates were smoothed over a window of 10 Mb with a shift of 1 Mb. The three maps coincide well. The calculation of the normalized recombination rates is described in Materials and methods.

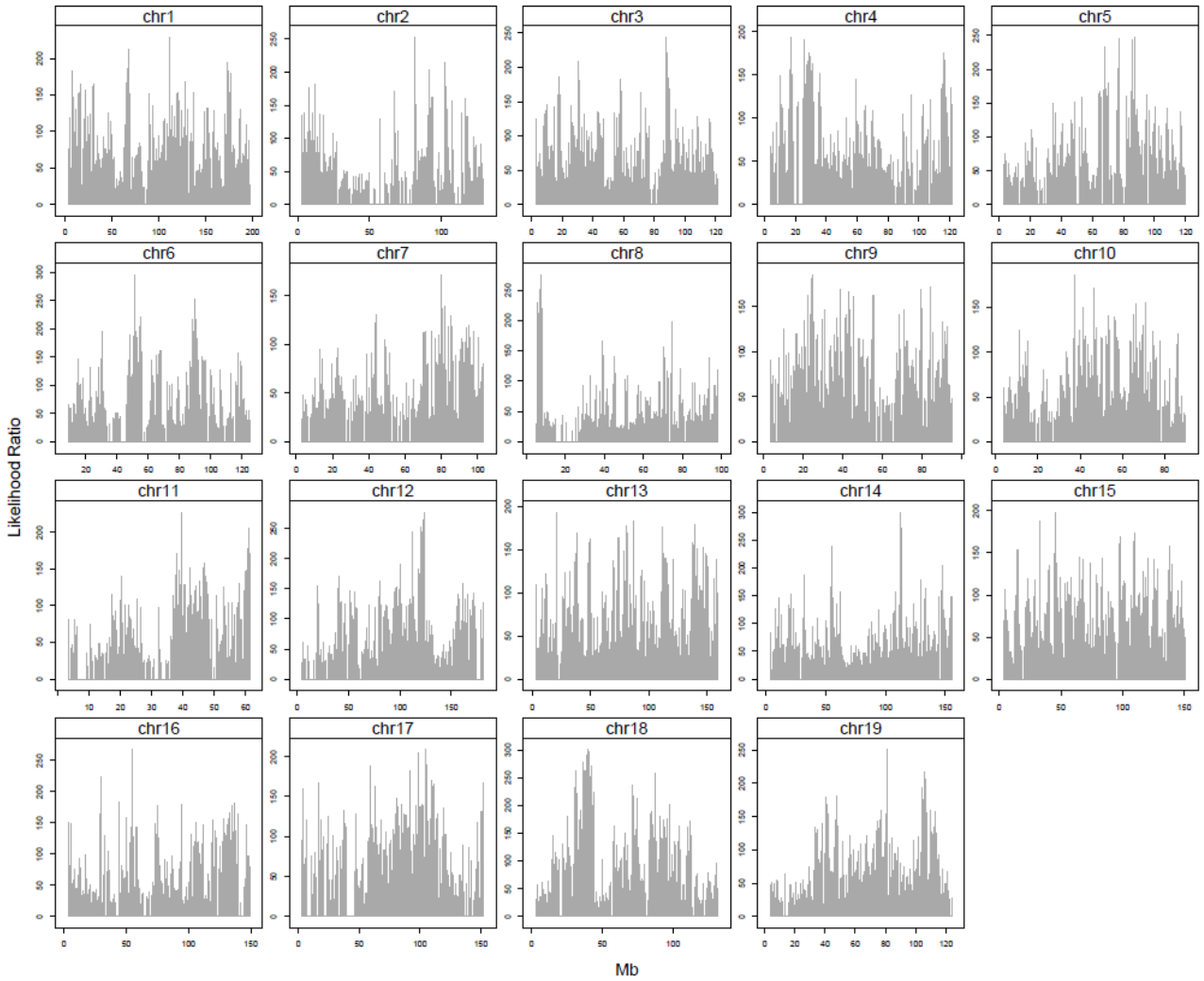

Figure S8 Distribution of hotspots along chromosomes. Each vertical bar is a hotspot. The heights of the bars are the likelihood ratios, evidence of the existence of a hotspot as output by sequenceLDhot.

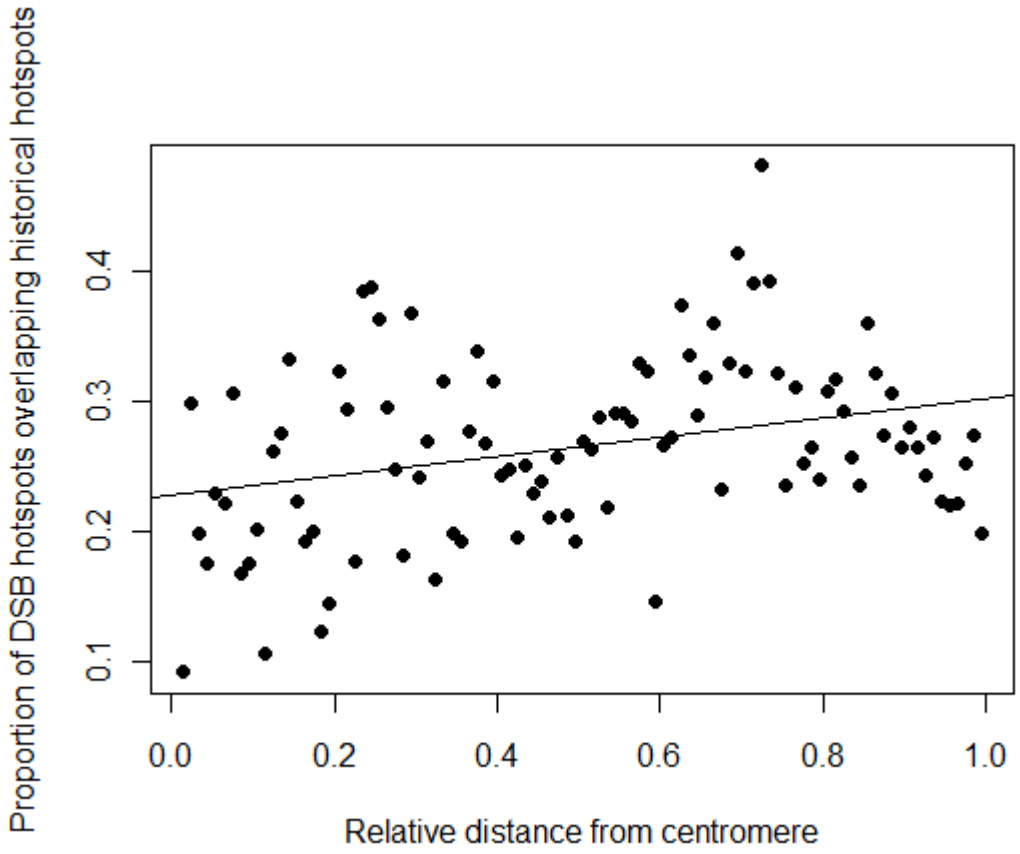

Figure S9 The relationship between the relative distance from the centromere and the probability for DSB hotspots to overlapping historical hotspot. The relative distance from the centromere was calculated for each chromosome as the proportion of the chromosome length. DSB hotspots were divided into 100 bins based on the relative distance from the centromere.

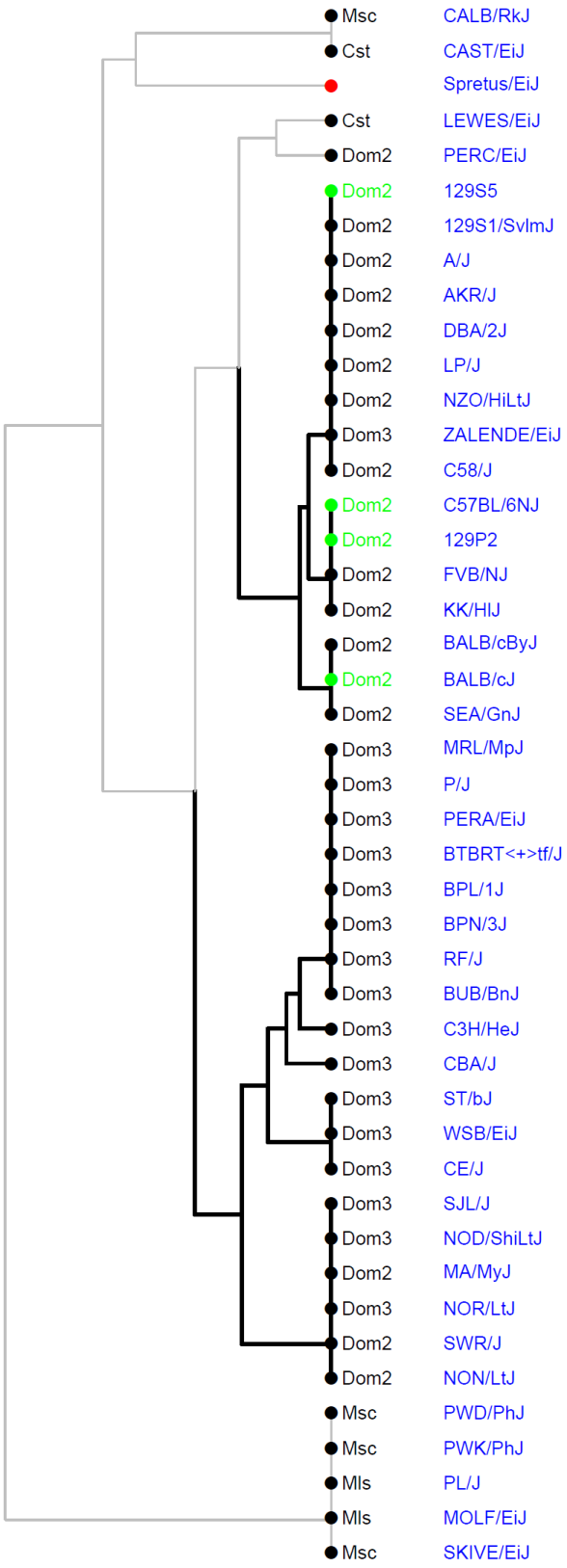

Figure S10 *Prdm9* alleles in 95 mouse inbred strains (Cst, Dom2, Dom3, Msc, Mls). *Prdm9* alleles were genotyped or imputed using SNPs in a 5kb window surrounding the *Prdm9* gene. Next to each strain (names in blue) is the group assignment. The group assignments for strains which have been sequenced at *Prdm9* are shown in black. Imputed genotypes are shown in green. Imputation for one strain was unsuccessful (red bullet). The two largest clusters are Dom2 and Dom3 (shown in bold lines).

Tables S1 and S2

Supporting Tables

Tables S1 and S2 are available for download at http://www.genetics.org/content/suppl/2012/05/04/genetics.112.141036.DC1 as .csv files.

Table S3 Individual repeats and repeat families that are significantly enriched in hotspots.

	Hotspots	Coldspots	P-value*	Relative Risk
Repeat Family				
Simple_repeat	20025	18157	6.33E-20	1.103
Low_complexity	10146	9562	0.00171	1.061
L1	12842	12285	0.0235	1.045
Individual Repeats				
L1Md_F2	1739	1138	3.35E-26	1.528
MTA_Mm	616	366	1.52E-12	1.683
L1Md_T	501	290	6.55E-11	1.728
GC_rich	335	186	7.45E-08	1.801
GA-rich	1757	1399	2.23E-07	1.256
L1Md_F3	453	291	3.48E-06	1.557
L1Md_A	350	211	5.31E-06	1.659
MTA_Mm-int	122	51	7.58E-05	2.392
L1_Mus1	794	595	0.000115	1.334
L1Md_F	128	62	0.00214	2.065
B1_Mus2	2520	2202	0.00439	1.144
Simple Repeats				
(GA)n	2942	1780	1.24E-61	1.653
(TC)n	2858	1764	1.20E-55	1.62
(TA)n	2916	1829	1.98E-53	1.594
(CA)n	5986	5114	1.48E-13	1.171
(GAAA)n	715	452	1.50E-11	1.582
(TG)n	5961	5153	2.10E-11	1.157
(T)n	1283	948	1.56E-09	1.353
(TTTC)n	672	442	6.44E-09	1.52
(A)n	1302	977	1.18E-08	1.333
(GGAA)n	434	272	1.3E-06	1.596
(TCTA)n	660	467	0.000011	1.413
(GAA)n	304	189	0.00028	1.608
(TTTTC)n	234	137	0.000603	1.708

* P-value corrected using Bonferroni correction

Table S4 List of strains from different sources and their known Prdm9 alleles.

Original 17	Sequenced in this study	Sequenced by Parvanov [S4]	Combined
129P2/OlaHsd			*NA*
129S1/SvImJ		129S1/SvImJ	Dom2
129S5SvEvBrd			*NA*
A/J		A/J	Dom2
AKR/J		AKR/J	Dom2
BALB/cJ			*NA*
C3H/HeJ		C3H/HeJ	Dom3
C57BL/6NJ			*NA*
CAST/EiJ		CAST/EiJ	Cst
CBA/J	CBA/J	CBA/CaJ	Dom3
DBA/J	DBA/2J	DBA/2J	Dom2
LP/J	LP/J		Dom2
NOD/ShiLtJ	NOD/LtJ	NOD/LtJ	Dom3
NZO/HlLtJ	NZO/HILtJ	NZO/HlLtJ	Dom2
PWK/PhJ		PWK/PhJ	Msc
SPRET/EiJ			*NA*
WSB/EiJ		WSB/EiJ	Dom3
	SJL/J		Dom3
	CALB/RkJ		Msc
	ST/bJ		Dom3
	P/J		Dom3
	PERC/EiJ		Dom2
	CE/J		Dom3
	MRL/MpJ		Dom3
	PERA/EiJ	PERA/EiJ	Dom3
	ZALENDE/EiJ		Dom3
	BTBRT<+>tf/J		Dom3
	C58/J		Dom2
	BPL/1J		Dom3
	BPN/3J		Dom3
	PL/J		Mls
	MA/MyJ		Dom2
	RF/J		Dom3
	FVB/NJ	FVB/NJ	Dom2
	SKIVE/EiJ	SKIVE/EiJ	Msc
	KK/HiJ	KK/HiJ	Dom2
	NOR/LtJ		Dom3
	SWR/J		Dom2
	NON/LtJ		Dom2
	LEWES/EiJ		Cst
	SEA/GnJ		Dom2
	BuB/BnJ		Dom3
		PWD/PhJ	Msc
		BALB/cByJ	Dom2
		MOLF/EiJ	Mls

NA = Unkown *Prdm9* allele

SUPPORTING REFERENCES

S1. Cox A. et al., *Genetics* **182**, 1335-1344 (2009).

S2. Paigen K. et al., PLoS Biology **7**(2), 340-349 (2009).

S3. Billings T. et al., *PLoS One* **5(12)**, e15340 (2010).

S4. Parvanov, E.D., P.M. Petkov, and K. Paigen. *Science* **327:** 835 (2010).